



Carbon nanobeads as an anode material on high rate capability lithium ion batteries

Jian-Chia Chang^a, Yu-Fen Tzeng^b, Jin-Ming Chen^c, Hsin-Tien Chiu^b, Chi-Young Lee^{a,d,*}

^a Department of Materials Science and Engineering, National Tsing Hua University, Hsinchu, Taiwan, ROC

^b Department of Applied Chemistry, National Chiao Tung University, Hsinchu, Taiwan, ROC

^c Industrial Technology Research Institute Hsinchu, Taiwan, ROC

^d Center of Nanotechnology, Materials Science, and Microsystem, National Tsing Hua University, Hsinchu, Taiwan, ROC

ARTICLE INFO

Article history:

Received 30 March 2009

Received in revised form 3 July 2009

Accepted 4 July 2009

Available online 15 July 2009

Keywords:

Rechargeable lithium battery

Carbonaceous anode

High rate capability

ABSTRACT

Carbon nanobeads (CNBs) were prepared by reacting cyclohexachlorobenzene with dispersed sodium metal at 200 °C for 4 h. The CNBs prepared in this manner formed uniform nanobeads, with sizes ranging from 100 to 300 nm. Heating resulted in a reduction in the size of the CNBs, and improvements in their degree of crystallinity. The nanosized carbon materials considerably increased the surface area of the powder, reducing the distance of the intercalation/deintercalation pathway, substantially improving the charge capacity of the lithium ion battery at a high charging rate. The charge capacity of CNBs was found to be 238 mAh g⁻¹, while that of commercial MCMB reached only 36 mAh g⁻¹, when the charging rate was 1C (372 mAh g⁻¹). As the charging rate was further increased to 2C (744 mAh g⁻¹) and 3C (1116 mAh g⁻¹), the charge capacities of CNBs dropped to 173 and 111 mAh g⁻¹, respectively. The cyclic performance of the CNBs was measured and found to be significantly improved in comparison to other carbonaceous materials, for up to 100 cycles. Although cyclic performance did result in a gradual reduction in capacity, the CNBs still greatly exceeded the capacity of MCMB. These results clearly demonstrate the potential role of CNBs as anodes for high capacity Li ion batteries for use in the automobile industry.

© 2009 Elsevier Ltd. All rights reserved.

1. Introduction

Lithium ion batteries have received increasing interest in recent years. Owing to their high energy density, lightweight design and environmental friendliness, these batteries have become the favored power source for consumer electronic devices, such as cellular phones and laptop computers. Despite their impressive commercial success, lithium ion batteries must be further improved to enable them to meet the demands of ongoing market innovations.

The range of applications for lithium ion batteries can be extended to the automotive industry only by improving the charging/discharging rate of the batteries to provide a high power density. The limitation on the charging rate of lithium ion batteries is widely believed to be associated with the slow solid-state diffusion of lithium ions in active electrode materials [1]. A practical means of increasing the apparent diffusivity of lithium ions in the active materials is to reduce the particle size [2]. However, decreasing

the particle size increases the reactivity between the electrode and the electrolyte. Martin et al. demonstrated that the capabilities of nanostructured SnO₂ and V₂O₅ electrodes that were prepared using a template method were better than those of thin-film controlled electrodes [3–7]. These results support the conclusion that the improved rate capability is associated with a shorter solid-state diffusion path in the nanostructured materials.

Carbonaceous materials are presently the preferred material for producing anodes in rechargeable lithium batteries because they exhibit both increased specific capacity and a more negative redox potential than metal oxides, chalcogenides and polymers. The quality of lithium intercalation and deintercalation depends strongly on the crystalline phase, microstructure and micro-morphology of the carbonaceous materials [8,9].

This work presents a simple method for making CNBs at low temperature. This form of carbon supports the high charging rate and good cycle performance of the anode in a lithium ion battery.

2. Experiments

Sodium dispersed in paraffin wax (Sigma–Aldrich) was used as the starting material. It was soaked in a Teflon container with C₆Cl₆ (cyclohexachlorobenzene, Aldrich) and then sealed inside a stainless steel autoclave. The molar ratio of sodium dispersed in paraffin

* Corresponding author at: Department of Materials Science and Engineering, National Tsing Hua University, 101, Sec. 2, Kung Fu Rd., Hsinchu, Taiwan, ROC. Tel.: +886 3 5728692; fax: +886 3 5166687.

E-mail address: cylee@mx.nthu.edu.tw (C.-Y. Lee).

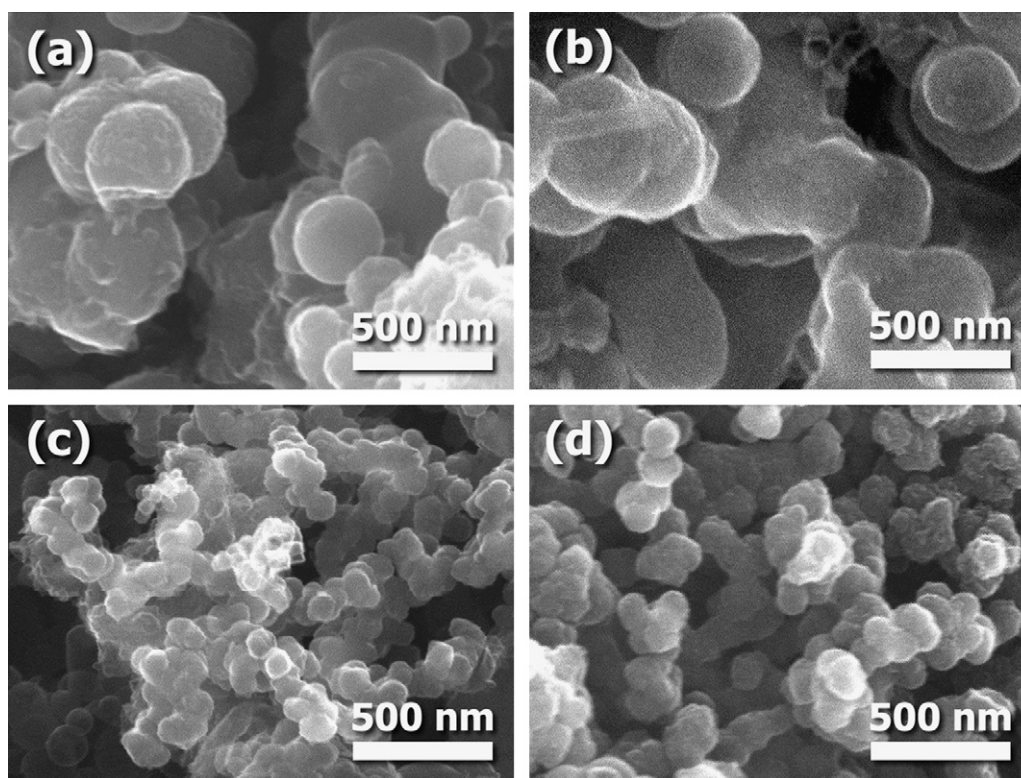


Fig. 1. SEM images of carbon nanobeads treated at different temperatures. (a) C-200, (b) C-1000, (c) C-1500 and (d) C-2000.

wax: C_6Cl_6 was 6:1. The solvent thermal treatment was performed by placing the autoclave in an oven at a temperature of about $200^\circ C$ for 4 h, and then allowing it to cool to room temperature in air. The product was filtered, then washed with hexane several times to remove the wax and with distilled water to remove residual NaCl. Then, the precipitates were dried at $110^\circ C$ for 2 h. The CNBs were further heat-treated at 1000, 1500 and $2000^\circ C$ for 30 min in a stream of highly pure argon.

The surface morphologies of the powders were observed under a JEOL 6500 field emission scanning electron microscope (FESEM) that was equipped with an energy dispersive X-ray spectrometry system (EDS) to detect elements. TEM images were obtained using a JEOL-2010 electron microscope. The structure of the produced CNBs was elucidated by X-ray diffraction (Bruker D8-advanced diffractometer with $CuK\alpha$ radiation). The degree of graphitization of the carbon was observed by Raman spectroscopy.

The electrochemical cells were comprised of a CNBs-based composite as the negative electrode, lithium metal as the counter electrode and an electrolyte of 1M $LiPF_6$ in ethylene carbonate (EC)/ethyl methyl carbonate (EMC)/propylene carbonate (PC)/dimethyl carbonate (DMC) (vol% of 3:4:1:2). The cell separator was a Celgard 2400 membrane. The anode was a mixture of 83 wt% carbon active material and 17% polyvinylidene fluoride (PVDF) as a binder. The cell was assembled in an argon-filled dry box. All of the electrochemical tests were conducted at room temperature. Charge/discharge cycle tests were performed using Arbin BT2000 at a constant current density, with a cutoff voltage of 1.8–0.01 V.

3. Results and discussions

A black powder was synthesized by reacting C_6Cl_6 with dispersed sodium metal at $200^\circ C$ for 4 h. The powder was then heated at 200, 1000, 1500 or $2000^\circ C$ —denoted C-200, C-1000, C-1500 and C-2000, respectively, and the morphologies, compositions,

microstructures and lithium ion intercalation properties were studied.

Fig. 1 presents the SEM micrographs of the CNBs, C-200, C-1000, C-1500 and C-2000. The SEM observations indicated that the morphologies of the powders comprised strings of uniformly sized beads. The sizes of the as-prepared powder and those heated below $1000^\circ C$ were about 200 nm. When the heating temperature exceeded $1500^\circ C$, the CNBs shrank to approximately 100 nm beads. According to the EDS analysis, the as-prepared powder and powder heated below $1000^\circ C$ consisted of C, Na and Cl. When the heat-treatment temperature exceeded $1000^\circ C$, carbon was the only element in the powder. The presence of Na and Cl may have been associated with the formation of NaCl during the reaction of Na with C_6Cl_6 , which was removed when the powder was heated at over $1000^\circ C$.

The degree of graphitization of C-200, C-1000, C-1500 and C-2000 was identified by XRD, as displayed in Fig. 2a. When the heating temperature was less than $1000^\circ C$, the major peaks of the products at about $2\theta = 31.8, 45.6$ and 56.7 were assigned to the (110), (111) and (200) planes of NaCl and a broad peak at around 26° was assigned to the (002) planes of the somewhat amorphous carbon materials. The detection of NaCl is consistent with the result of the composition study. Treatment at over $1500^\circ C$ markedly increased the intensity of the peak at 26° . The value of the parameter L_c , evaluated from the line widths of the peak at 26° , was adopted to estimate the degree of crystallinity of the samples in the c -direction. The measured L_c values of C-1000, C-1500 and C-2000 are 8.59, 9.09 and 25.64 Å, respectively, revealing that a higher heat-treatment temperature results in better crystallinity in the c -direction of the carbon materials.

The graphene in-plane ordering of C-200, C-1000, C-1500 and C-2000 was quantified using Raman scattering spectra to investigate the correlation between the extent of lithium ion intercalation and the crystallinity of the powders. The average I_D/I_G ratio, evalu-

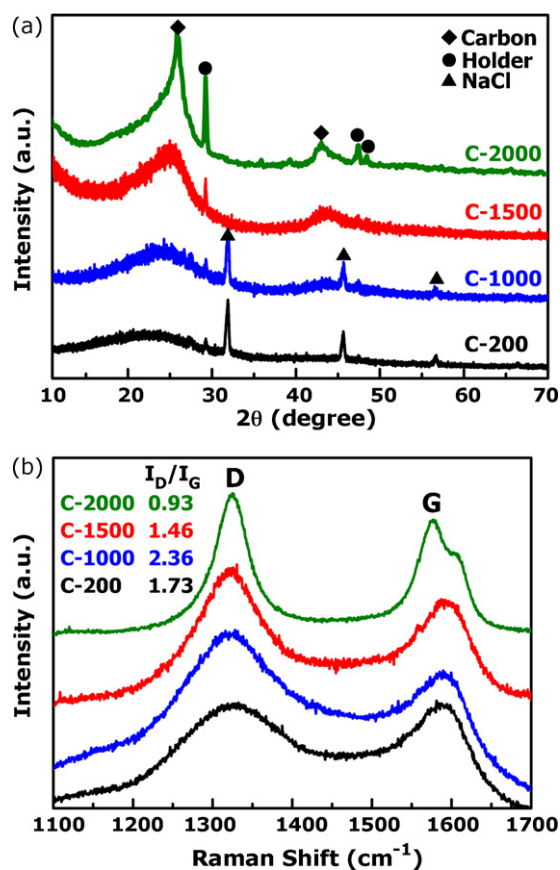


Fig. 2. (a) XRD and (b) Raman spectra of different heat-treated carbon nanobeads.

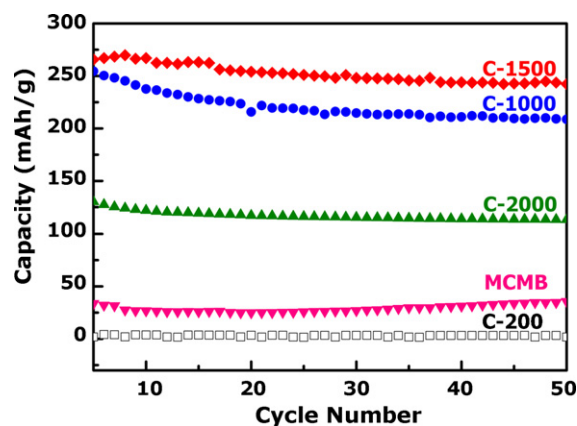


Fig. 4. Cycle ability of lithium ion batteries using different kinds of carbon nanobeads and MCMB as anodes at the current density 372 mAh g^{-1} .

ated from the integrated intensities of the D-band (defect-induced mode, near 1350 cm^{-1}) and G-band (graphite-related mode, at $1550\text{--}1605 \text{ cm}^{-1}$), is employed herein to determine the degree of crystallinity of the samples. Fig. 2b exhibits the Raman spectra of C-200, C-1000, C-1500 and C-2000. The La of C-2000 was 45 \AA , revealing a well-developed graphite structure. The La of other samples with less ordering is estimated to be in the range of $17\text{--}31 \text{ \AA}$. C-200 had the highest I_D/I_G ratio, revealing an amorphous carbon phase.

Fig. 3 displays the charge and discharge characteristics of the CNBs examined at a charging rate of 1C (372 mAh g^{-1}). The charge–discharge performance of the C-200, C-1000 and C-1500 is similar to that of the anodes made from typical carbon materials with a low degree of graphitization. Highly graphitized CNBs (C-2000) are similar to typical graphite materials, although the reversible capacity (124 mAh g^{-1}) is far lower than the theoretical capacity of graphite (372 mAh g^{-1}). The potential plateau between

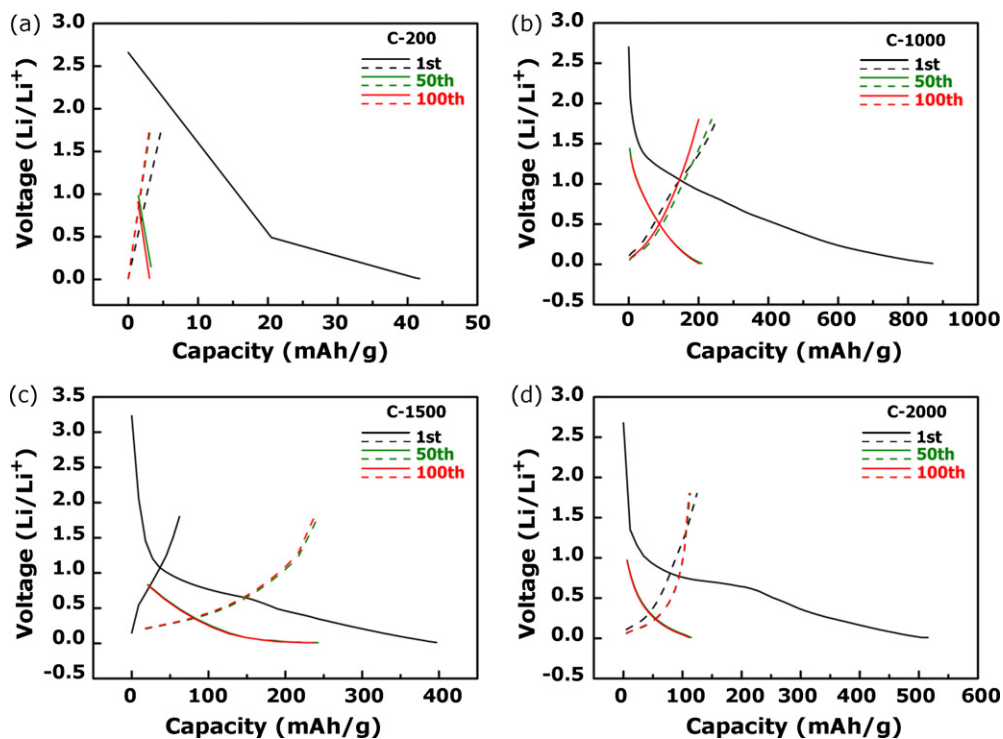


Fig. 3. Charge–discharge profiles of CNBs treated at different temperatures as lithium ion battery anodes at a charge–discharge current density of 1C (372 mAh g^{-1}). (a) C-200, (b) C-1000, (c) C-1500 and (d) C-2000.

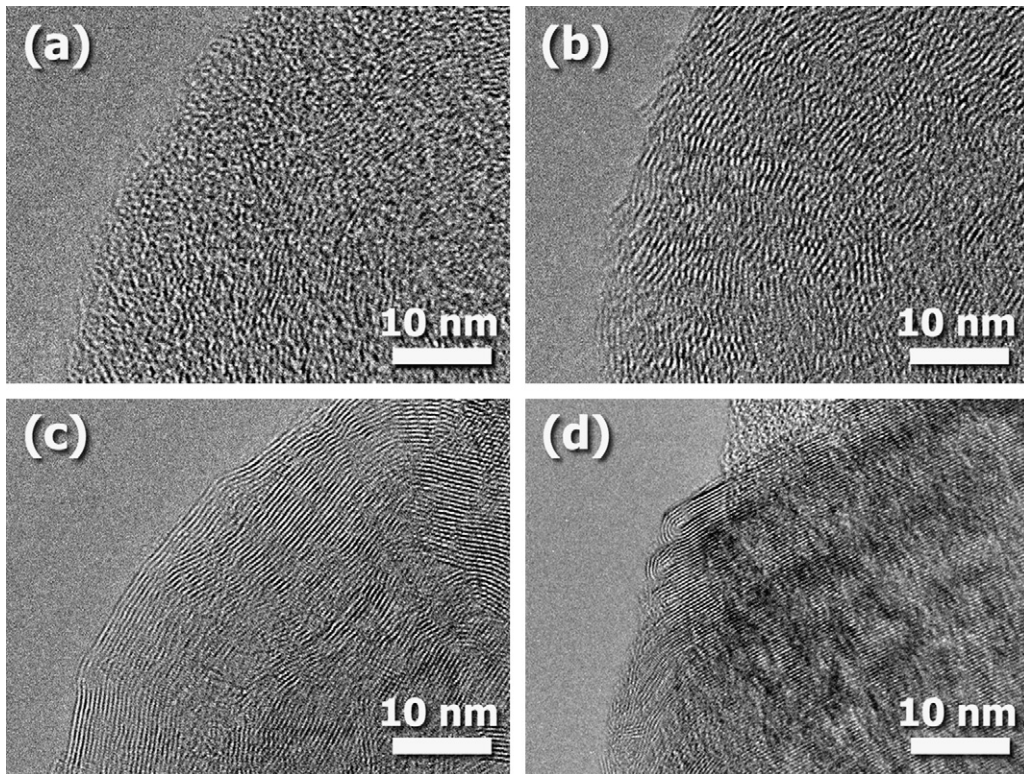


Fig. 5. HR-TEM images of carbon nanobeards treated at different temperatures. (a) C-200, (b) C-1500, (c) C-2000 and (d) MCMB.

0.7 and 1.0V against the ratio Li^+/Li , found only at the first charge cycle, is associated with the decomposition of electrolyte to form a solid electrolyte interface (SEI) film on the surface of the CNB electrode. The irreversible capacity at the first cycle is around 392 mAh g^{-1} , because of the formation of SEI. The nanosized carbon materials substantially increase the surface area of the powder, increasing the reactivity between the electrode and the electrolyte, generating SEI. The irreversible capacity declines markedly after the second cycle. The irreversible capacities in the first cycle for all the CNBs are as high as that following heat treatment at 2000°C , probably because of the nanostructure and similarity between the surface areas of these CNBs. However, reducing the particle size can reduce the distance through which the lithium ions must diffuse.

Therefore, a very high capacity can still be obtained with a high current density (372 mAh g^{-1}).

Fig. 4 shows the cycle behaviors of C-200, C-1000, C-1500, C-2000 and MCMB at the current density of 372 mAh g^{-1} (1C). The reversible capacities of all the samples gradually decreased during the first few cycles, and then remained almost constant. The reversible capacity of MCMB at 30 mAh g^{-1} was considerably lower than that at the current density of 37.2 mAh g^{-1} (0.1C), consistent with the previous observation [10]. The reversible capacity of C-200 is approximately zero because the nanostructure is responsible for the high irreversible capacity in the first cycle, since low graphitization is not associated with a site for lithium ions to insert/extract reversibly. As the heat-treatment temperature of the carbon materi-

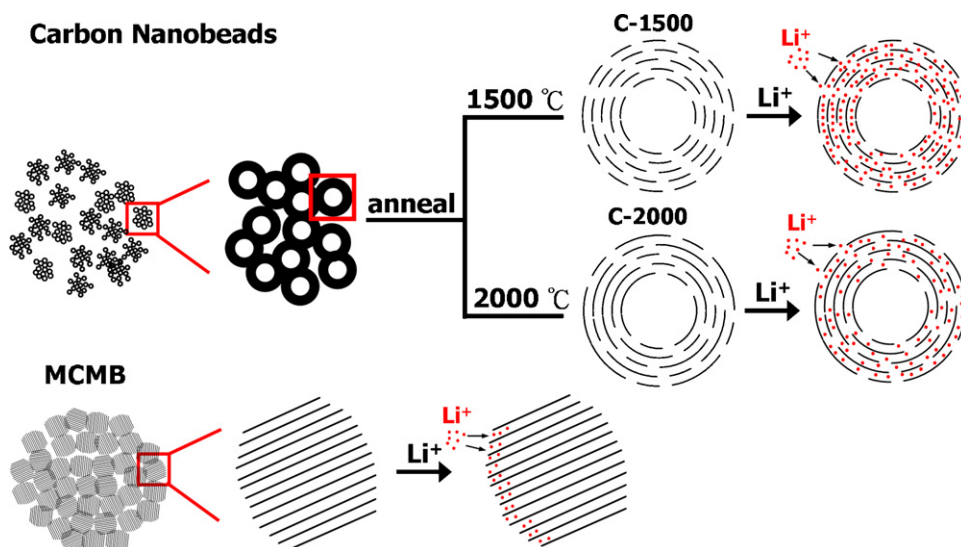


Fig. 6. Charge/discharge mechanism of MCMB and carbon nanobeards.

Table 1
1st charge/discharge capacities and efficiency of heat-treated carbon nanobeads. 100th cycle reversible capacities and capacity rate after 100 cycles.

	1st cycle charge capacity (mAh g ⁻¹)	1st cycle discharge capacity (mAh g ⁻¹)	1st cycle efficiency (%)	100th cycle reversible capacity (mAh g ⁻¹)	Capacity decay rate after 100 cycles (%)
C-200-2C	98.99	3.85	3.88	1.93	49.88
C-1000-2C	502.91	147.41	29.31	97.87	33.61
C-1500-2C	798.61	200.26	25.07	172.62	13.81
C-2000-2C	381.46	133.09	34.89	84.38	36.59
C-200-3C	100.25	4.25	4.24	2.12	50.12
C-1000-3C	231.64	51.92	22.41	85.09	–
C-1500-3C	533.44	130.65	24.49	111.31	14.81
C-2000-3C	423.99	94.58	22.31	81.41	13.92

als increases, the reversible capacity increases because the degree of graphitization increases. The reversible capacity was largest when the anode was made from CNBs that had been treated at 1500 °C. However, the CNB heated at 2000 °C had the largest La and Lc, but a poor reversible capacity. The low capacity of the C-2000 is probably associated with the high crystallinity of CNBs.

Fig. 5 reveals the transmission electron microscopic (TEM) images of C-200, C-1500, C-2000 and MCMB. TEM indicates that the C-200 is amorphous carbon without clear carbon layers. Upon heating to a high temperature, the degree of graphitization of the powders obviously improved and the carbon layers became clear. Heating at 2000 °C caused the powder to exhibit a high degree of graphitization, yielding graphene with few defects, as displayed in Fig. 5c. However, the high degree of crystallinity did not result in good performance of lithium ion batteries, because the complete graphite layer with a close end easily obstructed the intercalation/deintercalation of lithium ions into the graphene layers.

MCMB is a commercial anode material used for lithium ion batteries. It has near-theoretical reversible capacity, as determined at low current density. However, at high current density (372 mAh g⁻¹), the C-1000, C-1500 and C-2000 were found to have higher reversible capacities (208, 242 and 113 mAh g⁻¹, respectively) than MCMB (36 mAh g⁻¹) after 50 cycles. Fig. 6 schematically illustrates the charge/discharge pathway of CNBs and MCMB. The MCMB has high crystalline large particles, associated with many active sites, improving the intercalation/deintercalation of lithium ions. However, at high current density, the large particles are responsible for the length of the diffusion path associated with lithium ion intercalation/deintercalation, causing lithium ion intercalation/deintercalation to fail over a short period. While the lithium ions can be inserted into the internal active sites of the CNBs, the length of the path along which the lithium ions diffuse into the CNBs is short. Although the degree of graphitization of CNBs is lower than that of MCMB, CNBs markedly outperformed MCMB as an anode with a high rate capability for use in a lithium ion battery.

At high current density (2C = 744 mAh g⁻¹ and 3C = 1116 mAh g⁻¹), the cycle performance of the CNBs was similar to, but slightly lower than, that at a current density of 372 mAh g⁻¹ (1C). Table 1 presents the results. The capacity of C-200 with 2C is about 1.93, similar to that with 1C. C-1000, C-1500 and C-2000 also have high capacities of 97, 172 and 84 mAh g⁻¹, respectively, at 2C, and 85, 111 and 81 mAh g⁻¹, respectively at 3C, after 100 cycles.

4. Conclusions

This work identifies, for the first time, the high rate capability of CNBs as anode materials for lithium ion batteries. The highest rate capability is obtained when the CNBs are heat-treated at 1500 °C. The performance evaluated for 100 cycles was very good. These results demonstrate that CNBs have great potential for use as anodes in lithium ion batteries that are intended for use at high charging rates.

Acknowledgements

The authors would like to thank the National Science Council of the Republic of China, Taiwan, for financially supporting this research under Contract No. NSC 96-2113-M-007-021-MY3.

References

- [1] P.R. Bueno, E.R. Leite, *J. Phys. Chem. B* 107 (2003) 8868.
- [2] H. Wang, T. Abe, S. Maruyama, Y. Iriyama, Z. Ogumi, K. Yoshikawa, *Adv. Mater.* 17 (2005) 2857.
- [3] C.R. Sides, C.R. Martin, *Adv. Mater.* 17 (2005) 125.
- [4] C.J. Patrissi, C.R. Martin, *J. Electrochem. Soc.* 148 (2001) A1247.
- [5] N.C. Li, C.R. Martin, B. Scrosati, *J. Power Sources* 97 (8) (2001) 240.
- [6] N.C. Li, C.R. Martin, *J. Electrochem. Soc.* 148 (2001) A164.
- [7] C.J. Patrissi, C.R. Martin, *J. Electrochem. Soc.* 146 (1999) 3176.
- [8] M. Winter, J.O. Besenhard, M.E. Spahr, P. Novak, *Adv. Mater.* 10 (1998) 725.
- [9] M. Winter, J.O. Besenhard, in: M. Wakihara, O. Yamamoto (Eds.), *Ion Batteries: Fundamentals and Performance*, Wiley-VCH, Weinheim, 1998.
- [10] H. Wang, T. Abe, S. Maruyama, Y. Iriyama, Z. Ogumi, K. Yoshikawa, *Adv. Mater.* 17 (2005) 2857.